

Study on the interaction of kojic acid with tyrosinase by spectroscopic methods

DOI: 10.25177/JCCMM.4.2.RA.10607

Research

Accepted Date: 10th Mar 2020; Published Date: 20th Mar 2020

Copy rights: © 2020 The Author(s). Published by Sift Desk Journals.

This is an Open Access article distributed under the terms of the Creative Commons Attribution License

[\(http://creativecommons.org/licenses/by/4.0/\)](http://creativecommons.org/licenses/by/4.0/), which permits unrestricted use, distribution, and reproduction in any medium, provided the original work is properly cited.**Xue You¹, Cailian Wang¹, Nihong Guo¹, Wenbin Liu^{1*}**

¹ Department of Pharmaceutical and Biological Engineering, School of Chemical Engineering, Sichuan University, Chengdu 610065, China

CORRESPONDENCE AUTHOR

Wenbin Liu,

Tel: 86-28-85408255

E-mail: wbliu@scu.edu.cn

CITATION

Xue You, Cailian Wang, Nihong Guo, Wenbin Liu W, Study on the interaction of kojic acid with tyrosinase by spectroscopic methods(2020) Journal of Computational Chemistry & Molecular Modeling 4(2) pp:365-375

ABSTRACT

Tyrosinase is the key enzyme in melanin synthesis, and kojic acid is a widely available inhibitor against tyrosinase with extensive application values. The inhibitory mechanism of kojic acid was elaborated by studying the mutual interaction and the effects on tyrosinase conformation using spectroscopy. Ultraviolet-visible absorption spectra showed kojic acid caused both the secondary and tertiary structure changed. Fluorescence lifetime measurements implied that kojic acid quenched the intrinsic fluorescence of tyrosinase via static process. A complex formed through one single binding site with a binding constant of $1.35 \times 10^5 \text{ M}^{-1}$. Thermodynamic parameters suggested that the binding was a spontaneous process with hydrogen bonds and van der Waals forces playing main role. Synchronous fluorescence spectra and three-dimensional fluorescence spectra showed that kojic acid induced obvious conformational changes in tyrosinase and increased the polarity of microenvironment. Circular dichroism revealed an increase of the content of α -helix and β -strand. This study will provide reliable basis concerning the inhibitory mechanism of kojic acid against tyrosinase, and therefore contribute to development of tyrosinase inhibitor.

Keywords: Tyrosinase; Kojic acid; Inhibitory mechanism; Spectroscopy; Conformation

1. INTRODUCTION

Tyrosinase is widely distributed in organisms with an important role in melanin biosynthesis. Tyrosinase is the key enzyme for pigmentation of skin, wound healing, and molting process and immunity in insects [1]. However, overproduction of melanin could cause considerable problems, such as melanoma. Moreover, tyrosinase is also involved in the unfavorable food browning reaction. Therefore, the tyrosinase inhibitors therefore have been extensively applied in the field of cosmetics, food, pharmaceuticals, and agriculture [1]. Based on the safety apprehension, it is decisive to elaborate the inhibitory mechanism for the applications of tyrosinase inhibitors.

Kojic acid, a secondary metabolite produced by *Aspergillus* and *Penicillium*, has emerged as a cosmetic agent with an excellent skin lightener effect and also as a food preservative to prevent browning due to inhibitory effect on tyrosinase [2]. Kojic acid is usually served as the positive control to discover new tyrosinase inhibitors [1]. Previous studies only focus on the inhibitory effect and kinetic analysis [3,4]. However, the inhibitory mechanism and structure-activity relationship have been seldom explored in-depth so far. There is little knowledge on the modulation of the overall structures of tyrosinase involved in the inhibition by kojic acid. The gap between plenty of documents on inhibitory activity and lack of knowledge on inhibitory mechanism is striking for that well-known tyrosinase inhibitor, which has become an obstacle for development of potent lead compounds and the further application. It is urgent to further study the inhibitory mechanism of kojic acid towards to tyrosinase with respect to mutual interaction and conformational changes.

Given the structure of kojic acid, it was hypothesized that inhibition of tyrosinase activity by kojic acid resulted from conformational changes due to the interaction. In this study, the mechanism of tyrosinase inhibition was systematically investigated via examining the effects of kojic acid on tyrosinase structure, as well as the potential binding through the multispectroscopic studies. Binding mechanism was proposed. Three-dimensional fluorescence spectra and synchro-

nous fluorescence spectra technique were performed to evaluate the conformational effect. This research provided qualitative understanding of the regulation of tyrosinase activity at the molecular level. The results could provide some important theoretic information for various industrial applications of kojic acid as tyrosinase inhibitor.

2. MATERIALS AND METHODS

2.1. Materials

Mushroom tyrosinase was purchased from Worthington (New Jersey, USA). Tyrosinase was dissolved with potassium phosphate buffer (0.05 M, pH 6.5). Kojic acid (purity > 98%) was purchased from Jinsui Bio-Technology (Shanghai, China).

2.2. Ultraviolet-visible spectra measurements

The MAPAD UV-3100PC spectrophotometer (Shanghai, China) was employed to measure the Ultraviolet-visible (UV-Vis) absorption using quartz cuvette with 1.0 cm path length. Scans of absorption spectra were collected at 25°C. Differential spectra were obtained by subtracting the corresponding spectra from the spectra of the mixture.

2.3. Fluorescence spectra measurements

Steady state fluorescence spectra were carried out on a Shimadzu spectrofluorophotometer RF-6000 (Kyoto, Japan). All measurements were performed in a standard quartz cell of 1.0 cm path length, embedded in a thermostatic cell holder. Fluorescence emission spectra were recorded upon excitation wavelength at 280 nm. The slit widths for excitation and emission were set to 3 nm and 5 nm, respectively. A 3 ml solution in cuvette containing of 0.65 μM tyrosinase, within the linear concentration region for fluorescence intensity (data not shown), was added successively with 1 μl of 30 mM kojic acid aliquot using a trace syringe for 10 times. The addition of small volume of buffer solution during titration had little effect on the extent of fluorescence quenching [5,6]. Fluorescence quenching was analyzed by Stern-Volmer equation (1) [7,8]:

$$\frac{F_0}{F} = 1 + k_q \tau_0 [Q] = 1 + K_{sv} [Q] \quad (1)$$

where F_0 and F represent the fluorescence intensities

of tyrosinase without and with kojic acid, respectively; The inner filter effect was corrected[7]; k_q is the quenching rate constant; K_{sv} denotes the Stern-Volmer quenching constant; τ_0 is the average lifetime of the unquenched fluorophore ($\tau_0=10^{-8}$ s); and $[Q]$ is the concentration of kojic acid.

The equilibrium between free and bound molecules is described by equation (2)[9]:

$$\lg \frac{F_0 - F}{F} = \lg K_b + n \lg [Q] \quad (2)$$

where K_b is the binding constant; and n is the number of binding sites.

2.4. Time-resolved fluorescence lifetime measurements

Time-resolved fluorescence lifetime was examined with a Horiba Jobin Yvon Fluorolog-3 spectrofluorometer (Longjumeau, France) using 10 mm quartz cuvette. The excitation wavelength and the emission wavelength were fixed at 280 nm and 334 nm, respectively. The concentration of tyrosinase was kept fixed at 0.4 μM , whereas the concentration of kojic acid varied from 0 to 60 μM . The fluorescence decay curves were analyzed by triexponential iterative fitting program. The average fluorescence lifetime $\langle t_{AV} \rangle$ was calculated from the lifetimes (t_i) and preexponential factors (α_i) by using the following relationship (3):

$$\langle t_{AV} \rangle = \sum_i \alpha_i \tau_i \quad (3)$$

2.5. Electrochemical measurements

The electrochemical experiments were conducted through a Chenhua CHI660C electrochemical workstation (Shanghai, China). Three-electrode electrochemical system was employed, including a bare nickel electrode as the working electrode, an Hg/Hg₂Cl₂ electrode as the reference electrode, and a graphite rod as the counter electrode. PBB buffer serve as electrolyte. Tyrosinase and kojic acid solution at different concentrations was directly added into 20 mL electrolyte. Each measurement of cyclic voltammetry followed stirring for 3 min and resting for 2 min. The scan range was set from -0.6 to 0.6 V with a scan rate of 50 mV s⁻¹.

2.6. Thermodynamic parameters

If temperature varies in a limited range, the thermodynamic parameters, including enthalpy change (ΔH), entropy change (ΔS) and Gibbs free energy change (ΔG), could be evaluated on the basis of the equation (4) and equation (5)[10-12].

$$\lg K_b = -\frac{\Delta H}{2.303RT} + \frac{\Delta S}{2.303R} \quad (4)$$

$$\Delta G = \Delta H - T\Delta S \quad (5)$$

where R is the gas constant; T is the experimental temperature in Kelvin.

2.7. Synchronous and three-dimensional fluorescence spectra

Synchronous fluorescence spectra were gained with a fixed interval ($\Delta\lambda$) between excitation and emission wavelength at 25°C. Tyrosinase (0.65 μM) was titrated by increasing concentrations of kojic acid from 0 μM to 200 μM with increment of 10 μM each time. The emission wavelength were recorded from 245 nm to 385 nm (for $\Delta\lambda=15$ nm) and from 200 nm to 340 nm (for $\Delta\lambda=60$ nm), at which the spectrum could only show the characteristic information of Tyr and Trp residues of tyrosinase, respectively[13].

In order to measure the three-dimensional fluorescence, different concentrations of kojic acid were incubated with 0.65 μM tyrosinase. Excitation wavelengths from 225 to 350 nm and emission wavelengths from 280 to 450 nm were scanned at 25°C.

2.8. Circular dichroism spectra measurements

Circular dichroism (CD) spectra were collected using an Applied Photophysics Chirascan CD spectrometer (Leatherhead, UK) by a 1 mm path length quartz cuvette, which was attached with a Peltier type temperature control system. Far-UV CD spectrum was examined at wavelength in the range from 185 nm to 250 nm at a bandwidth of 2nm. 300 μL tyrosinase (1 μM) was incubated with 1 μL various concentration of kojic acid (0, 1, 4 μM) at for 1 minutes, and then was measured at 25°C. The contents for different secondary structures of tyrosinase were quantitatively analyzed by the online CDSSTR program with Set 4 as the reference set[14,15].

2.9. Data process

All assays were individually repeated in triplicate. For the sake of clarity, error bars were not shown. Origin[®] 8.1 was used for data process.

3. RESULTS AND DISCUSSION

3.1. Ultraviolet-visible spectra for interaction between kojic acid and copper ion or tyrosinase

It was reported that the ability to chelate copper ion exerts an enormous function on the tyrosinase inhibition[4]. The direct interaction of kojic acid with the copper ion was revealed by the UV-Vis spectra of kojic acid treated with gradually increasing concentrations of copper ion (Figure 1A). The peak at 217 nm and 269 nm for kojic acid shifted to 223 nm and 309 nm, respectively. The characteristic red shift suggested the formation of chelate between copper ion and kojic acid[4,16,17]. Isobestic points mirrored the existence of free and bound forms of kojic acid in equilibrium (Figure 1A). The chelation between kojic acid and copper ion in the enzyme was also investigated (Figure 1B). In contrast to a bathochromic shift for copper ions in solution, no significant wavelength

shift was observed after incubation with tyrosinase (Figure 1B). Therefore, the inhibitory mechanism of kojic acid differed from those of simple copper chelators[4,18].

UV-Vis absorption spectroscopy is also an effective method to examine the formation of complex as well as the structural alteration[15,17]. The UV-Vis absorption spectra of tyrosinase in the absence and presence of kojic acid were shown in Fig. 1B. The increased intensity of the differential spectrum for tyrosinase suggested binding of kojic acid to tyrosinase as well as changes in conformation of the protein skeleton[5,20]. Transformation of secondary structure made the polypeptide strand more extended and induced global conformational change. Furthermore, the weak absorption bands around 280 nm seemed to slightly shift towards shorter wavelength upon addition of kojic acid, demonstrating that the interaction of kojic acid with tyrosinase decreased the hydrophobicity of the microenvironment surrounding Trp residues.

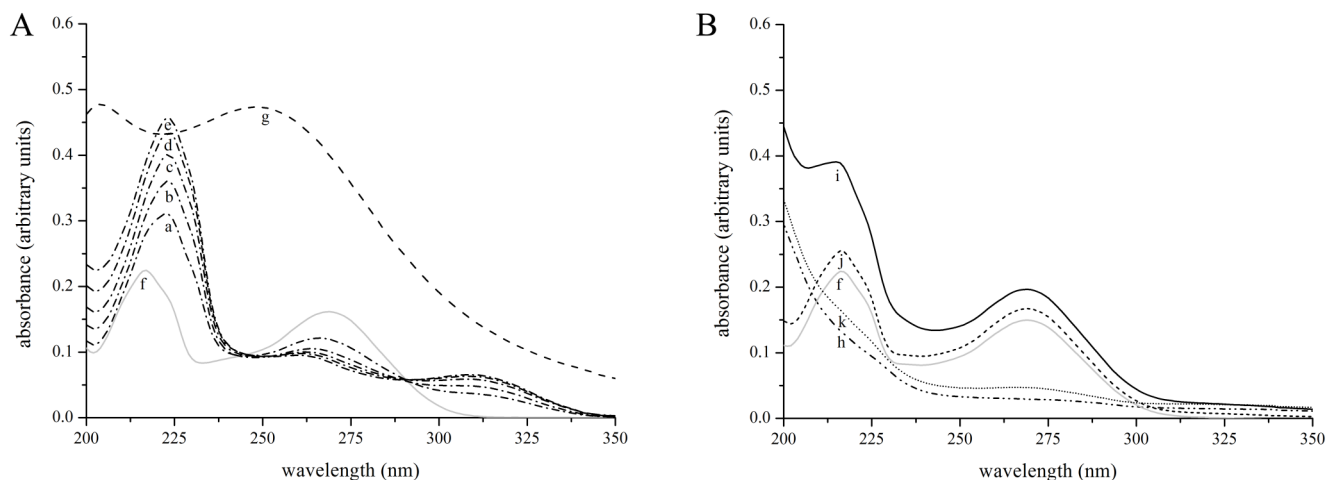


Figure 1. Ultraviolet-visible spectra of kojic acid. (A) Absorption spectrum for kojic acid (0.02 mM) upon addition of various concentration of copper ion. Kojic acid was incubated with 0.02, 0.04, 0.06, 0.08, and 0.10 mM CuSO₄. Dash-dot line a to e – 0.02 mM kojic acid with 0.02, 0.04, 0.06, 0.08, and 0.10 mM CuSO₄; Gray line f – 0.02 mM kojic acid; Dashed line g – 0.10 mM CuSO₄. (B) Absorption spectrum for kojic acid (0.02 mM) upon addition of tyrosinase (90 nM). Differential absorption spectra were obtained by deducting the corresponding spectra from the spectrum of the mixture. Dash-dot-dot line h – 90 nM tyrosinase; Black line i – 90 nM tyrosinase with 0.02 mM kojic acid; Short dashed line j – differential absorption spectra by deducting tyrosinase; Short dash-dot line k – differential absorption spectra by deducting kojic acid.

Table 1: Quenching constants and thermodynamic parameters for the interaction between kojic acid and tyrosinase

T (K)	K_{sv} ($\times 10^4 M^{-1}$)	k_q ($\times 10^{10} M^{-1} s^{-1}$)	K_b ($\times 10^5 M^{-1}$)	n	ΔH (kJ mol $^{-1}$)	ΔS (J mol $^{-1} K^{-1}$)	ΔG (kJ mol $^{-1}$)
288	4.54	45.42	1.35	1.11			-22.70
298	3.36	33.61	0.70	1.08	-40.04	-60.31	-22.10
310	2.56	25.56	0.41	1.06			-21.38

3.2. Fluorescence quenching of interaction between kojic acid and tyrosinase

Tyrosinase at a fixed concentration was titrated by gradual addition of kojic acid (Figure 2). It was apparent that successive addition of kojic acid led to a regular decrease in the fluorescence intensity of tyrosinase without discernable shift of the maximum peak wavelength. Approximately 60% of the fluorescence was quenched when the concentration of kojic acid reached 100 μM .

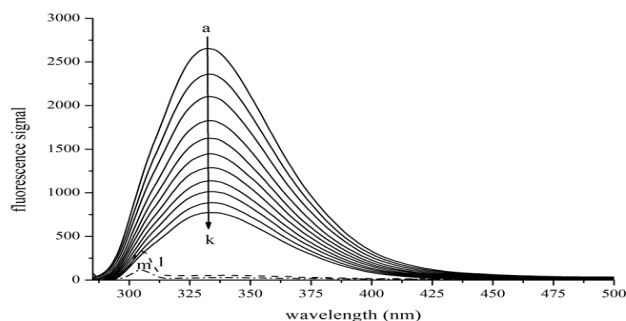


Figure 2: Intrinsic fluorescence changes in the presence of various kojic acid concentrations. Tyrosinase at concentration of 0.65 μM was titrated by kojic acid and then incubated for 30 seconds before measurement. Solid lines a to k – emission spectra of 0.65 μM tyrosinase titrated by 0, 10, 20, 30, 40, 50, 60, 70, 80, 90, 100 μM kojic acid at 298 Kelvin; Dashed line l – potassium phosphate buffer solu-

tion; Dash-dot line m – emission spectrum of 200 μM kojic acid alone.

To explain the probable mechanism for quenching, the fluorescence quenching at three temperatures was carried out, including 288, 298, and 310 Kelvin (Figure 3A). The Stern-Volmer plot displayed a good linear relationship under the concentration range, suggesting that only a single quenching type occurred[7,12,19]. The k_q values at different temperatures appeared much larger than the maximum diffusion collision quenching rate constant ($2 \times 10^{10} M^{-1} s^{-1}$) (Table 1)[7,9,21]. In addition, the corresponding K_{sv} values, which decreased with the rising temperature, were inversely correlated with temperature. Therefore, it was confirmed that quenching of tyrosinase by kojic acid might be mainly governed by a static quenching procedure[7,9,21]. It was concluded that a specific interaction most likely took place and a ground-state complex without fluorescence was possibly formed.

Figure 3B showed the resulting double-logarithm curves. The K_b value was calculated to be $1.35 \times 10^5 M^{-1}$ at 298 K (Table 1), suggesting that kojic acid exhibited relatively strong binding affinity toward tyrosinase. The values of n was approximately close to 1, and thus indicated the presence of just a single binding site on tyrosinase[12,23].

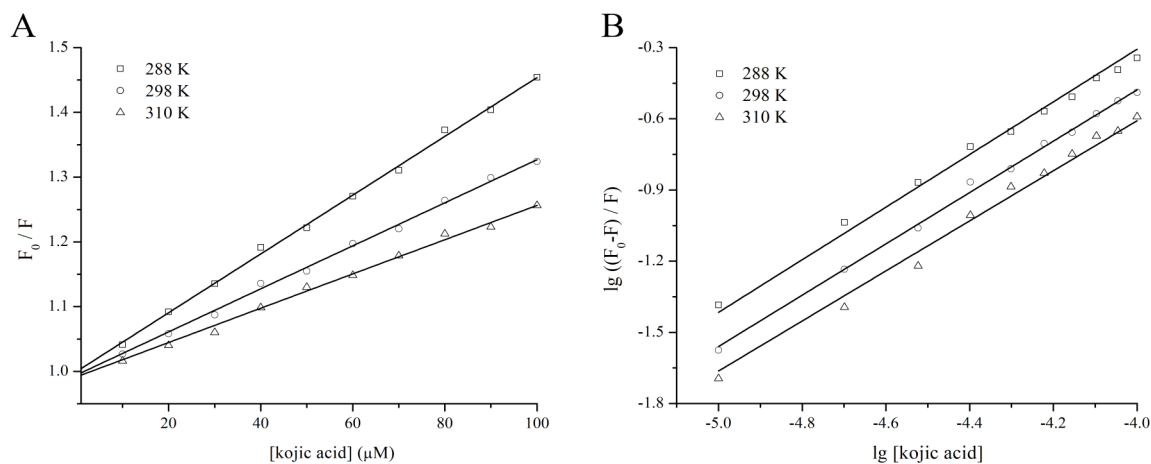


Figure 3: Fluorescence quenching effect of kojic acid on tyrosinase at different temperatures. (A) Stern-Volmer plots for the quenching at different temperatures. Open square (\square) – 288 Kelvin; Open circle (\circ) – 298 Kelvin; Open triangle (\triangle) – 310 Kelvin; [Kojic acid] – concentration of kojic acid; F_0 – fluorescence intensities of tyrosinase without kojic acid; F – fluorescence intensities of tyrosinase with kojic acid; lg – logarithm. (B) Double-logarithm plots for the quenching at different temperatures.

Table 2: Fluorescence lifetime of tyrosinase as a function of concentration of kojic acid.

	t_1 (ns)	t_2 (ns)	t_3 (ns)	α_1	α_2	α_3	t_{AV} (ns)	χ^2
Tyrosinase	2.18	0.53	5.37	0.38	0.52	0.10	1.64	1.129
Tyrosinase + kojic acid (3 μ M)	2.12	0.53	5.24	0.38	0.52	0.10	1.61	1.107
Tyrosinase + kojic acid (15 μ M)	2.22	0.55	5.44	0.38	0.53	0.09	1.63	1.083
Tyrosinase + kojic acid (30 μ M)	2.18	0.53	5.37	0.38	0.53	0.09	1.61	1.072
Tyrosinase + kojic acid (60 μ M)	2.13	0.52	5.30	0.39	0.51	0.10	1.61	1.058
Tyrosinase + kojic acid (90 μ M)	2.19	0.53	5.38	0.38	0.52	0.09	1.62	1.080

3.3. Fluorescence lifetimes

The type of quenching mechanism could be directly identified by fluorescence lifetime[7,12]. The fluorescence decay of tyrosinase in the presence of different concentrations of kojic acid exhibited triexponential profiles with good fitting (Figure 4). Evidently, the fluorescence decay patterns scarcely changed after the addition of kojic acid. The average lifetime decreased slightly from 1.64 ns to 1.62 ns (Table 2), which could be considered null in the range of experimental error. These results further indicated that the quenching was really a static mode because a non-fluorescent complex was formed.

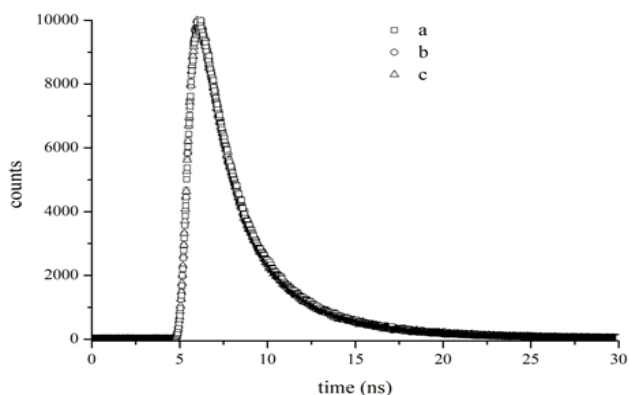


Figure 4: Representative time-resolved fluorescence decay profiles of tyrosinase at various molar ratios of kojic acid. Tyrosinase at concentration of 0.4 μ M was incubated by kojic acid (0, 15, 60 μ M) for 30 seconds before measurement. Open square (\square) a – 0.4 μ M tyrosinase; Open circle (\circ) b – 0.4 μ M tyrosinase with 15 μ M kojic acid; Open triangle (\triangle) c – 0.4 μ M tyrosinase with 60 μ M kojic acid.

3.4. Electrochemistry

Cyclic voltammetry could provide additional information on interaction mode[24]. The cyclic voltammogram of kojic acid in absence and presence of tyrosinase were monitored by keeping the concentration of tyrosinase constant while varying the concentration of kojic acid (Figure 5). The increment in intensities of the currents for increasing concentrations of kojic acid in presence of tyrosinase was lower than that in absence of tyrosinase, which was suggestive of the reduction of equilibrium concentration of free kojic acid in solution[25]. Thus, it could be concluded that a non-electroactive complex formed to block the electron transfer between kojic acid and electrode [24].

3.5. Thermodynamic parameters and interaction forces

Attention was focused on the acting force to interpret the binding mode (Figure 6 and Table 1). ΔG values were all negative, indicating that the spontaneity of the binding process[12,26]. The negative sign for ΔH revealed that the binding process was an exothermic reaction[26,27]. Based on the thermodynamic criterion[11], the negative ΔH and ΔS values meant that both hydrogen bond and van der Waals force played a main role in the binding process. In case of kojic acid, hydroxyl groups were easy to form intermolecular hydrogen bonds with the polar side chains of residues in the binding pocket[28]. The property of electronic configuration of kojic acid was advantage for van der Waals force to take part in the interaction[13].

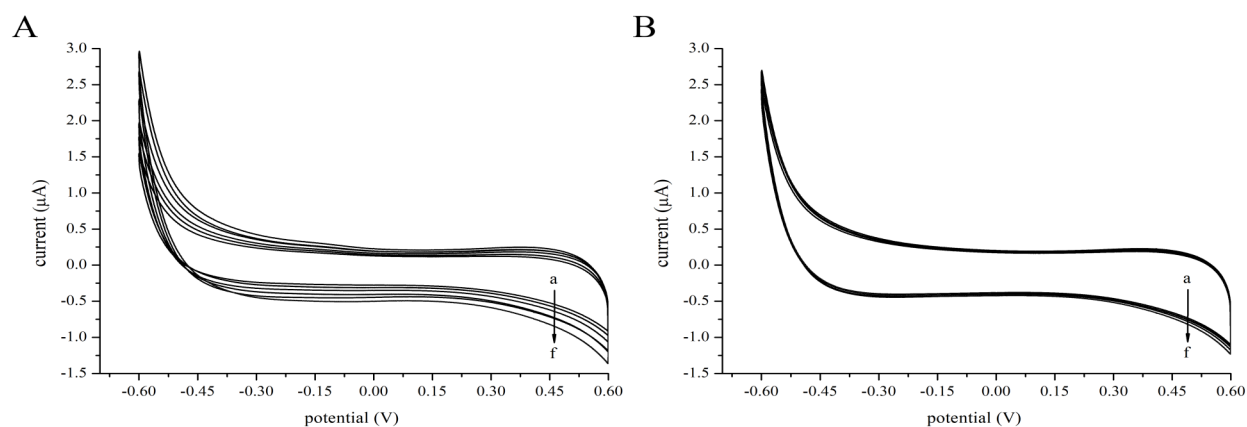


Figure 5: Cyclic voltammograms of kojic acid with tyrosinase. (A) Various concentrations of kojic acid in the absence of tyrosinase. The scan rate was 50 mVs^{-1} . Solid lines a to f – 0, 10, 20, 30, 40, 50 μM kojic acid. (B) Various concentrations of kojic acid in the presence of $1 \mu\text{M}$ tyrosinase.

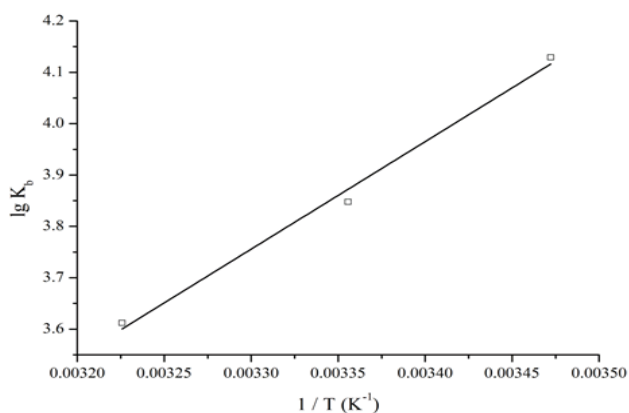


Figure 6: Van't Hoff plot. T – experimental temperature (Kelvin); lg – logarithm; K_b – binding constant

3.6. Conformational changes of tyrosinase upon binding of kojic acid

The synchronous fluorescence for $\Delta\lambda$ at 60 nm showed changes on the peak shape and a noticeable

red shift of spectral peak from 340 nm to 351 nm upon gradual addition of kojic acid (Figure 7A). The red shift suggested that binding of kojic acid exposed the Trp residues more to the solvent, and thus increased the hydrophilicity surrounding the Trp residues [10,28]. This finding corroborated the results obtained from UV-Vis absorption experiment. Comparatively, the synchronous fluorescence for $\Delta\lambda$ at 15 nm exhibited only very slightly red shift (Figure 7B), reflecting that kojic acid had little effect on the microenvironment around Tyr residues. Dramatic decrease in intensities was observed in both synchronous fluorescence spectra. The degree of quenching for $\Delta\lambda$ at 60 nm was higher than that at 15 nm, implying that kojic acid was probably located closer to Trp residue compared to Tyr residue [29]. The microenvironmental alterations of the Trp residues indicated that structure changes occurred after the interaction with kojic acid.

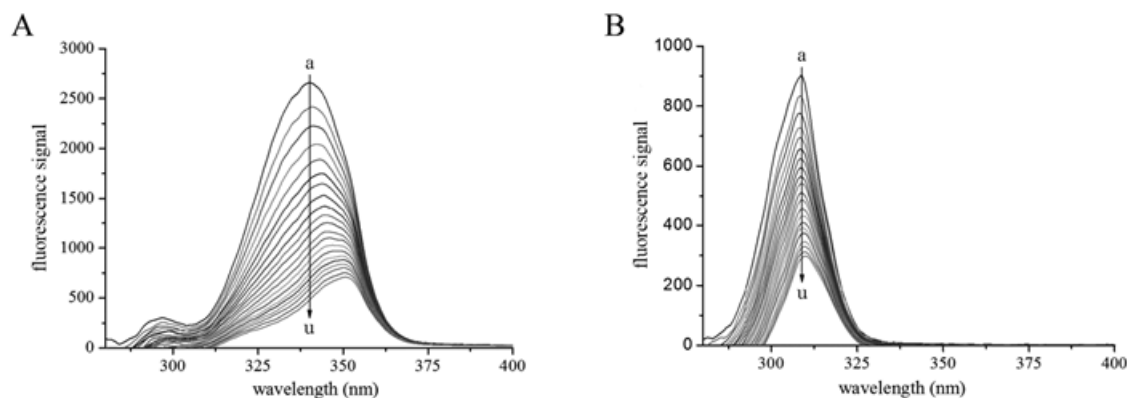


Figure 7: Synchronous fluorescence spectrum of tyrosinase titrated by kojic acid. (A) Interval between excitation and emission wavelength ($\Delta\lambda$) = 60 nm. Solid lines a to u – synchronous fluorescence spectrum of $0.65 \mu\text{M}$ tyrosinase titrated 0, 10, 20, 30, 40, 50, 60, 70, 80, 90, 100, 110, 120, 130, 140, 150, 160, 170, 180, 190, 200 μM kojic acid at 298 Kelvin. (B) $\Delta\lambda = 15 \text{ nm}$.

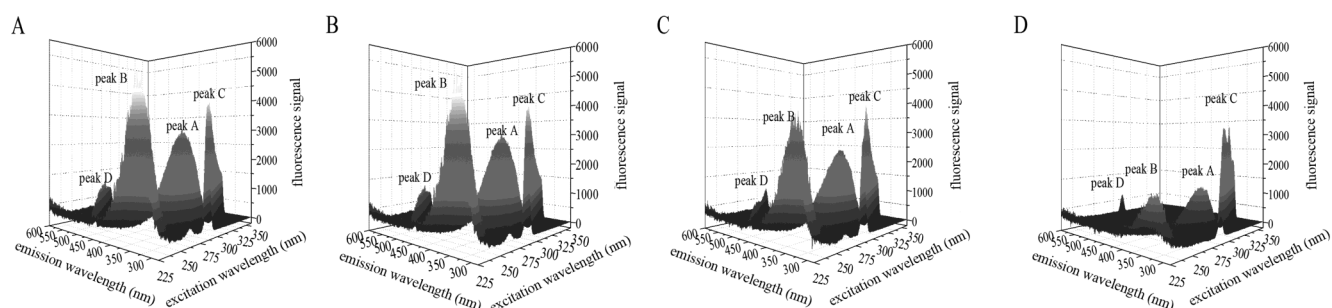


Figure 8: Three-dimensional fluorescence spectra of tyrosinase at different kojic acid concentrations. (A) Tyrosinase alone. peak A – intrinsic Trp and Tyr residues peak; peak B – polypeptide backbone peak; peak C – Rayleigh scattering peak; peak D – second-order scattering peak; [tyrosinase] = 0.65 μ M; temperature = 298 Kelvin. (B) Tyrosinase with 0.08 mM kojic acid. (C) Tyrosinase with 0.16 mM kojic acid. (D) Tyrosinase with 0.32 mM kojic acid.

Table 3: Characteristic parameters for three-dimensional fluorescence spectra of tyrosinase in presence of kojic acid.

kojic acid (mM)	peak A				peak B			
	peak position $\lambda_{ex}/\lambda_{em}$ (nm/nm)	fluorescence signal	$(F_0 - F) / F_0$ (%)	Stokes $\Delta\lambda^a$ (nm)	peak position $\lambda_{ex}/\lambda_{em}$ (nm/nm)	fluorescence signal	$(F_0 - F) / F_0$ (%)	Stokes $\Delta\lambda^a$ (nm)
0	280/333	2507	0	53	228/334	4256	0	106
0.08	286/333	2078	17.11	47	228/339	2321	45.47	111
0.16	291/337	1383	44.83	46	230/337	1375	67.69	107
0.32	294/336	649	74.11	42	233/346	556	86.94	113

^a Stokes $\Delta\lambda = \lambda_{em} - \lambda_{ex}$.

The modulation in the three dimensional fluorescence spectra upon kojic acid corresponded to the presence of binding in terms of the decrease of fluorescence intensity (Figure 8). The typical Rayleigh scattering peak (peak C) and the second-order scattering peak (peak D) seemed to be seldom affected[23,26]. Peak A was characterized by the spectral feature of both the intrinsic Trp and Tyr residues[23,26]. Peak B with the excitation wavelength around 230 nm essentially exhibited the fluorescence property of the polypeptide backbone structure of tyrosinase[23,26]. Kojic acid resulted in a decrement of fluorescence intensity for both peaks, with a more serious degree for peak B (Table 3). Moreover, the fluorescence quenching for peak A was accompanied with red shift of the maximum emission wavelength. It was drawn a conclusion that the environment around both residues became more polar[30,31]. The significant decrease of Stokes shift for peak A corroborated the abovementioned red shift. Thus it could be conjectured that interaction with kojic acid caused a major disturbance of the peptide backbone and improved the polarity of the microenvironment via exposing the hydrophobic regions[23,26].

The interaction of kojic acid with the secondary structure of tyrosinase was revealed by circular dichroism (Figure 9). Upon addition of kojic acid at increasing molar ratio, an increment of ellipticity was found for both two negative bands at 208 nm and 220 nm, indicating a slight gain of α -helix[22,23,31]. The proportions of different secondary structure compositions of tyrosinase were quantitatively estimated (Table 4) [12]. The content of α -helix increased from 30% in free tyrosinase to 36% at a molar ratio for kojic acid to tyrosinase of 4:1, while the content of β -strand increased from 17% to 21%. Some significant decrease was also observed for the content of β -turn and random coil. This results suggested that increase in the β -strand would lead to partial extending of polypeptide backbone and thus the conformation of tyrosinase became looser[32]. On the basis of the spectroscopic results above, it could be drawn a conclusion that the occupancy of active site by kojic acid could lead to destabilization of the native conformation of tyrosinase, followed by disruption of its biological activities[32,33].

Table 4: The contents of secondary structures of tyrosinase in the presence of kojic acid^a.

	α -Helix (%)	β -Strand (%)	β -Turns (%)	Random Coil (%)
Tyrosinase	30	17	23	30
Tyrosinase + kojic acid (1 μ M)	32	19	20	29
Tyrosinase + kojic acid (4 μ M)	36	21	18	25

^a: Tyrosinase at 1 μ M

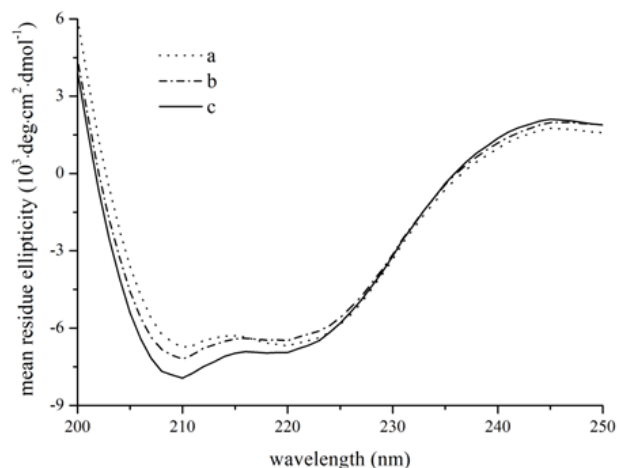


Figure 9: Circular dichroism spectra of tyrosinase at different kojic acid concentrations at 298 K. The concentration of tyrosinase was kept fixed at 1 μ M, the molar ratios of kojic acid to tyrosinase were 0:1, 1:1 and 4:1. Dot line a – 1 μ M tyrosinase; Dash-dot line b – 1 μ M tyrosinase with 1 μ M kojic acid; Black line c – 1 μ M tyrosinase with 4 μ M kojic acid.

4. CONCLUSIONS

The inhibitory mechanism of kojic acid on tyrosinase was disclosed by an integrated study on spectroscopy in this study for the first time. Kojic acid had a single class of binding sites on tyrosinase. A complex spontaneously formed between kojic acid and tyrosinase through static process. The binding constant was $1.35 \times 10^5 \text{ M}^{-1}$. The interaction caused global conformational changes of tyrosinase and thus increased the microenvironmental polarity. These experimental observations interpreted that kojic acid might inhibit the oxidation of L-DOPA via inducing conformational changes after binding to tyrosinase. The results obtained in this study provided a fresh insight into the relationship between activity and structure for tyrosinase regarding molecular recognition. It has a great significance in further design of safe and effective tyrosinase inhibitors.

COMPETING INTEREST

The authors declare that they have no competing interests.

AUTHOR'S CONTRIBUTIONS

W.L. designed the experiments. X.Y., and C.W. performed the experiments. X.Y., and N.G. analyzed the data. All authors wrote the manuscript.

ACKNOWLEDGEMENTS

This work was supported by the Strategic Partnership Funds of Sichuan University.

REFERENCES

- [1] Chang T S (2009) An Updated Review of Tyrosinase Inhibitors. *Int J Mol Sci* 10: 2440-2475. PMID:19582213 [View Article](#) [PubMed/NCBI](#)
- [2] Burnett C L, Bergfeld W F, Belsito D V, Hill R A, Klaassen C D, Liebler D C, Marks J G, Shank R C, Slaga T J, Snyder P W (2010) Final Report of the Safety Assessment of Kojic Acid as Used in Cosmetics. *Int J Toxicol* 29: 244S-273S. PMID:21164073 [View Article](#) [PubMed/NCBI](#)
- [3] Lima C R, Silva J R, De T C, Silva E O, Lameira J, Do Nascimento J L, Do Socorro Barros Brasil D, Alves C N (2014) Combined Kinetic Studies and Computational Analysis on Kojic Acid Analogous as Tyrosinase Inhibitors. *Molecules* 19: 9591-9605. PMID:25004069 [View Article](#) [PubMed/NCBI](#)
- [4] Kubo I, Kinshori I (1999) Flavonols from Saffron Flower: Tyrosinase Inhibitory Activity and Inhibition Mechanism. *J Agric Food Chem* 47: 4121-4125. PMID:10552777 [View Article](#) [PubMed/NCBI](#)
- [5] Copeland R A (1994) *Methods for Protein Analysis : a Practical Guide to Laboratory Protocols*;

- Chapman & Hall.
- [6] Zhang Q J, Liu B S, Li G X, Han R (2016) Using Resonance Light Scattering and UV/Vis Absorption Spectroscopy to Study the Interaction between Gliclazide and Bovine Serum Albumin. *Luminescence* 31: 1109-1114. PMID:26663583 [View Article](#) [PubMed/NCBI](#)
- [7] Lakowicz (2006) Principles of Fluorescence Spectroscopy, 3rd ed. Springer: New York. [View Article](#)
- [8] Pathak M, Mishra R, Agarwala P K, Ojha H, Singh B, Singh A, Kukreti S (2016). Binding of ethyl pyruvate to bovine serum albumin: Calorimetric, spectroscopic and molecular docking studies. *Thermochim Acta* 633: 140-148. [View Article](#)
- [9] Wei X L, Xiao J B, Wang Y, Bai Y (2009) Which Model Based on Fluorescence Quenching is Suitable to Study the Interaction between Trans-Resveratrol and BSA? *Spectrochim. Acta A Mol Biomol Spectrosc* 75: 299-304. PMID:19926336 [View Article](#) [PubMed/NCBI](#)
- [10] Huang Y, Yan J, Liu B, Yu Z, Gao X, Tang Y, Zi Y (2010) Investigation on Interaction of Prulifloxacin with Pepsin: A Spectroscopic Analysis. *Spectrochim Acta A Mol Biomol Spectrosc* 75: 1024-1029. PMID:20045662 [View Article](#) [PubMed/NCBI](#)
- [11] Ross P D, Subramanian S (1981) Thermodynamics of Protein Association Reactions: Forces Contributing to Stability. *Biochemistry* 20: 3096-3102. PMID:7248271 [View Article](#) [PubMed/NCBI](#)
- [12] Wang Y J, Zhang G W, Yan J K, Gong D M (2014) Inhibitory Effect of Morin on Tyrosinase: Insights from Spectroscopic and Molecular Docking Studies. *Food Chem* 163: 226-233. PMID:24912720 [View Article](#) [PubMed/NCBI](#)
- [13] Tu B, Chen Z F, Liu Z J, Li R R, Ouyang Y, Hu Y J (2015) Study of the Structure-Activity Relationship of Flavonoids Based on Their Interaction with Human Serum Albumin. *Rsc Adv* 5: 73290-73300. [View Article](#)
- [14] Whitmore L, Wallace B A (2008) Protein Secondary Structure Analyses from Circular Dichroism Spectroscopy: Methods and Reference Databases. *Biopolymers* 89: 392-400. PMID:17896349 [View Article](#) [PubMed/NCBI](#)
- [15] Guo N H, Wang C L, Shang C, You X, Zhang L Y, Liu W B (2018) Integrated Study of the Mechanism of Tyrosinase Inhibition by Baicalein Using Kinetic, Multispectroscopic and Computational Simulation Analyses. *Int J Biol Macromol* 118: 57-68. PMID:29908273 [View Article](#) [PubMed/NCBI](#)
- [16] Kim D, Park J, Kim J, Han C, Yoon J, Kim N, Seo J, Lee C (2006) Flavonoids as Mushroom Tyrosinase Inhibitors: A Fluorescence Quenching Study. *J Agric Food Chem* 54: 935-941. PMID:16448205 [View Article](#) [PubMed/NCBI](#)
- [17] Shang C, Zhang Y K, You X, Guo N H, Wang Y, Fan Y, Liu W B (2018) The Effect of 7,8,4'-Trihydroxyflavone on Tyrosinase Activity and Conformation: Spectroscopy and Docking Studies. *Luminescence* 33: 681-691. PMID:29479807 [View Article](#) [PubMed/NCBI](#)
- [18] Gao H, Nishida J, Saito S, Kawabata J (2007) Inhibitory Effects of 5,6,7-Trihydroxyflavones on Tyrosinase. *Molecules* 12: 86-97. PMID:17693955 [View Article](#) [PubMed/NCBI](#)
- [19] Pasricha S, Sharma D, Ojha H, Gahlot P, Pathak M, Basu M, Kukreti S (2017). Luminescence, circular dichroism and in silico studies of binding interaction of synthesized naphthylchalcone derivatives with bovine serum albumin. *Luminescence* 32: 1252-1262. PMID:28512990 [View Article](#) [PubMed/NCBI](#)
- [20] Huang J, Yuan Y Z, Liang H (2002) Binding Equilibrium Study of Phosphotungstic Acid and HSA or BSA with UV Spectrum, Fluorescence Spectrum and Equilibrium Dialysis. *Sci Chi Chem* 45: 200-207. [View Article](#)
- [21] Weert M V, Stella L (2011) Fluorescence Quenching and Ligand Binding: A Critical Discussion of A Popular Methodology. *J Mol Struct* 998: 144-150. [View Article](#)
- [22] Sharma D, Ojha H, Pathak M, Singh B, Sharma

- N, Singh A, Sharma R K (2016). Spectroscopic and molecular modelling studies of binding mechanism of metformin with bovine serum albumin. *J Mol Struct* 1118: 267-274. [View Article](#)
- [23] Peng W, Ding F, Jiang Y T, Sun Y, Peng Y K (2014) Evaluation of the Biointeraction of Colorant Flavazin with Human Serum Albumin: Insights from Multiple Spectroscopic Studies, in Silico Docking and Molecular Dynamics Simulation. *Food Funct* 5: 1203-1217. PMID:24705828 [View Article](#) [PubMed/NCBI](#)
- [24] Wang Y J, Zhang G W, Yan J K, Gong D (2014) Inhibitory Effect of Morin on Tyrosinase: Insights from Spectroscopic and Molecular Docking Studies. *Food Chem* 163: 226-233. PMID:24912720 [View Article](#) [PubMed/NCBI](#)
- [25] Magdum P A, Gokavi N M, Nandibewoor S T (2016) Study on the Interaction between Anti-Tuberculosis Drug Ethambutol and Bovine Serum Albumin: Multispectroscopic and Cyclic Voltammetric Approaches. *Luminescence* 32: 206-216. PMID:27377878 [View Article](#) [PubMed/NCBI](#)
- [26] Wang J, Xiang C, Tian F F, Xu Z Q, Jiang F L, Liu Y (2014) Investigating the Interactions of A Novel Anticancer Delocalized Lipophilic Cation and Its Precursor Compound with Human Serum Albumin. *RSC Adv* 4: 18205-18216. [View Article](#)
- [27] Ali M S, Al-Lohedan H A (2016) Multi-Technique Approach on the Interaction between Sugar-Based Surfactant N-Dodecyl B-D-Maltoside and Bovine Serum Albumin *J Lumin* 169: 35-42. [View Article](#)
- [28] Wang Y Q, Chen T T, Zhang H M (2010) Investigation of the Interactions of Lysozyme and Trypsin with Biphenol A Using Spectroscopic Methods. *Spectrochim Acta A Mol Biomol Spectrosc* 75: 1130-1137. PMID:20093070 [View Article](#) [PubMed/NCBI](#)
- [29] Ray D, Paul B K, Guchhait N (2012) Effect of Biological Confinement on the Photophysics and Dynamics of A Proton-Transfer Phototautomer: An Exploration of Excitation and Emission Wavelength-Dependent Photophysics of the Protein-Bound Drug. *Phys Chem Chem Phys* 14: 12182-12192. PMID:22870509 [View Article](#) [PubMed/NCBI](#)
- [30] Chen Z Y, Xu H Y, Zhu Y L, Liu J Y, Wang K Y, Wang P X, Shang S J, Yi X N, Wang Z L, Shao W (2014) Understanding The Fate of An Anesthetic, Nalorphine upon Interaction with Human Serum Albumin: A Photophysical and Mass-Spectroscopy Approach. *Rsc Adv* 4: 25410-25419. [View Article](#)
- [31] Samanta A, Paul B K, Guchhait N (2011) Spectroscopic Probe Analysis for Exploring Probe-Protein Interaction: A Mapping of Native, Unfolding and Refolding of Protein Bovine Serum Albumin by Extrinsic Fluorescence Probe. *Biophys Chem* 156: 128-139. PMID:21514035 [View Article](#) [PubMed/NCBI](#)
- [32] Mansouri M, Pirouzi M, Saberi M R, Ghaderabad M, Chamani J (2013) Investigation on the Interaction between Cyclophosphamide and Lysozyme in the Presence of Three Different Kind of Cyclodextrins: Determination of the Binding Mechanism by Spectroscopic and Molecular Modeling Techniques. *Molecules* 18: 789. PMID:23344194 [View Article](#) [PubMed/NCBI](#)
- [33] Ojha H, Mishra K, Hassan M I, Chaudhury N K (2012). Spectroscopic and isothermal titration calorimetry studies of binding interaction of ferulic acid with bovine serum albumin. *Thermochim acta*, 548, 56-64. [View Article](#)